JOURNAL OF APPLIED ELECTROCHEMISTRY 24 (1994) 149–156

Preparation and characterization of thin films of $LaNiO_3$ for anode application in alkaline water electrolysis

R. N. SINGH*, L. BAHADUR, J.P. PANDEY, S.P. SINGH

Electrochemical Laboratory, Department of Chemistry, Faculty of Science, Banaras Hindu University, Varanasi 221 005, India

P. CHARTIER, G. POILLERAT

Laboratoire d'Electrochimie et de Chimie-Physique du Corps Solide, URA au CNRS no. 405, Université Louis Pasteur, 4, rue Blaise Pascal, 67000 Strasbourg, France

Received 30 March 1993; revised 15 July 1993

$LaNiO_3$ electrodes were prepared, in the form of thin films on platinum by the methods of spray pyrolysis and sequential coating of mixed metal nitrate solutions followed by thermal decomposition. The films were adherent and of p-type semiconducting. Cyclic voltammetric studies indicated the formation of a quasireversible surface redox couple, Ni(III)/Ni(II), on these films before the onset of oxygen evolution in 1 M KOH. The anodic Tafel slopes were ~ 40 and $\sim 65\,mV\,decade^{-1}$, on the sprayed $LaNiO_3$ film and on the film obtained by a layer method, respectively. The reaction order with respect to OH^- was found to be 2.2 on the sprayed oxide film and 1.2 on the layer film. The sprayed oxide film was found to be electrocatalytically more active. It is suggested that the oxygen evolution reaction proceeds on both the film electrodes via the formation of the physisorbed H_2O_2 as an intermediate in the rate determining step.

1. Introduction

The increasing costs of fossil fuels and deleterious effects of their combustion products on the environment has produced considerable interests during recent years [1–7] in the development of alkaline water electrolysis cells for large scale hydrogen production, for use as a feed stock in specific applications such as fuel cells. Commercial electrolysers have only 70–80% efficiency [1], mainly due to the high oxygen evolving electrode activation overvoltages [6]. Normally, the electrolyte in water electrolysis cell is 20–30% (w/w) KOH, and in such media the preferred anode materials are nickel or nickel plated mild steel [1–7]. However, during use nickel anodes show an increase in overpotential [8, 9] with time, the increase being more at higher anodic potentials [8–10]. This decay in activity is probably due to the conversion of the electroactive species, Ni^{3+}, into an inactive species (Ni^{4+}) in the oxide layer [8, 11]. Efforts have been made to increase the efficiency of the traditional nickel anode [5, 12–15] and to develop cheaper and more stable anodes. Mixed oxides, particularly spinel-type [1, 6–22] or perovskite type [23–29], may be suitable candidate anodes in water electrolysis cells as they are of low cost, are highly active and have outstanding corrosion resistance in alkaline solutions under anodic conditions.

In recent years some perovskite-type anodes have been tested [23–29] from the standpoint of their activity as oxygen electrodes in alkaline solutions. Of the perovskite catalysts investigated, lanthanum nickelate, prepared by hydroxide coprecipitation, followed by thermal decomposition of the hydroxide residue, showed reasonably high activity [23–26]. The activity towards oxygen evolution [23] was reported to be ~ 50 times higher than that of the $NiCo_2O_4$ electrode and ~ 40 times higher than that of the nickel electrode in 1 M NaOH at 25° C. In these investigations, perovskite oxides were generally prepared by high temperature solid-state reactions of appropriate oxides, carbonates and oxalates etc. To produce higher surface area, other methods, such as freeze-drying [30] precipitation [31] and plasma jet spraying [32], have also been used. In each case the oxide electrodes used were in the form of pellets.

It is known [33] that the methodology, conditions and starting materials used in the preparation of oxides which are utilized in electrocatalysis affect their textural characteristics and hence their interfacial electrochemical properties. In view of this and to increase the electrical conductivity as well as the specific surface area and also to limit the amount of electroactive materials, we have obtained lanthanum nickelate in thin film forms on platinum substrate using the techniques of spray pyrolysis and sequential coating.

In this paper studies of the surface characterization of film electrodes and their electrocatalytic properties

* Author to whom correspondence should be addressed.

0021-891X

toward oxygen evolution in alkaline solutions are reported.

2. Experimental details

Commercial grade platinum foil (0.1 mm thick, 99.9% purity) was cut into 1 cm × 2 cm pieces, dipped into aqua regia for 15 min, washed thoroughly with distilled water, degreased in hot acetone, dried in air and then used for the preparation of oxide films.

In spray pyrolysis, equal volumes of aqueous solutions of 0.1 M $La(NO_3)_3.6H_2O$ and 0.1 M $Ni(NO_3)_2.6H_2O$ were mixed and 80 ml of the mixture was sprayed at a flow rate of $\sim 2\,ml\,min^{-1}$ onto platinum maintained at a constant temperature of 500° C. Air was used as the carrier gas and its pressure was maintained constant at 1 bar. Details of the experimental setup are given elsewhere [34]. After spraying, the coated platinum plate was further heated in a thermostatically controlled furnace at 700° C for 2 h.

In the second method, lanthanum and nickel nitrate solutions were prepared in ethanol and the concentration of both metal ions in the mixture was kept at 0.025 M. For the film preparation, one drop of the mixture was placed on one of the two faces of the support using a fine brush and uniformly spread over the whole surface. It was then allowed to dry in air. When the surface was dry, the second layer of solution was applied. This process was repeated 3 or 4 times to obtain the required catalyst loading ($\sim 9\,mg\,cm^{-2}$) on the platinum surface. Finally, the dried coated platinum plate was heated at 700° C for 2 h to obtain the $LaNiO_3$ film on platinum.

Electrical connection to the oxide film was made via the platinum surface not used for the film preparation. Only 1 cm × 1 cm area of the film was used for electrochemical studies: the remaining area, including the platinum surface, was covered with Araldite.

The formation of the desired oxide was confirmed through recording the X-ray diffraction pattern of the film as deposited on a quartz plate under similar experimental conditions. The morphology of the oxide surface was examined using a scanning electron microscope (Jeol).

The electrochemically active surface area of the electrodes was determined from double layer charging curves, using a cyclic voltammetric technique [24–26]. The Mott–Schottky plots and capacitance-potential curves were determined from the impedance measurements.

Electrochemical studies were carried out in a conventional three electrode Pyrex glass cell [18]. The potential of the working electrode was measured against a Hg–HgO–1 M KOH electrode; unless otherwise stated, all the potentials mentioned in the text are with respect to this reference which is 0.098 V vs SHE. The reference electrode was not brought into contact with the cell solution directly, but was connected through a Luggin capillary (KCl agar–agar salt bridge), the tip of which was placed as close as possible to the surface of the working electrode in order to minimize the solution resistance between test and reference electrode. The uncompensated solution resistance was determined by impedance measurements using an electrochemical impedance system (Model 378-3, EG&G PARC). 100 ml 1–4 M KOH

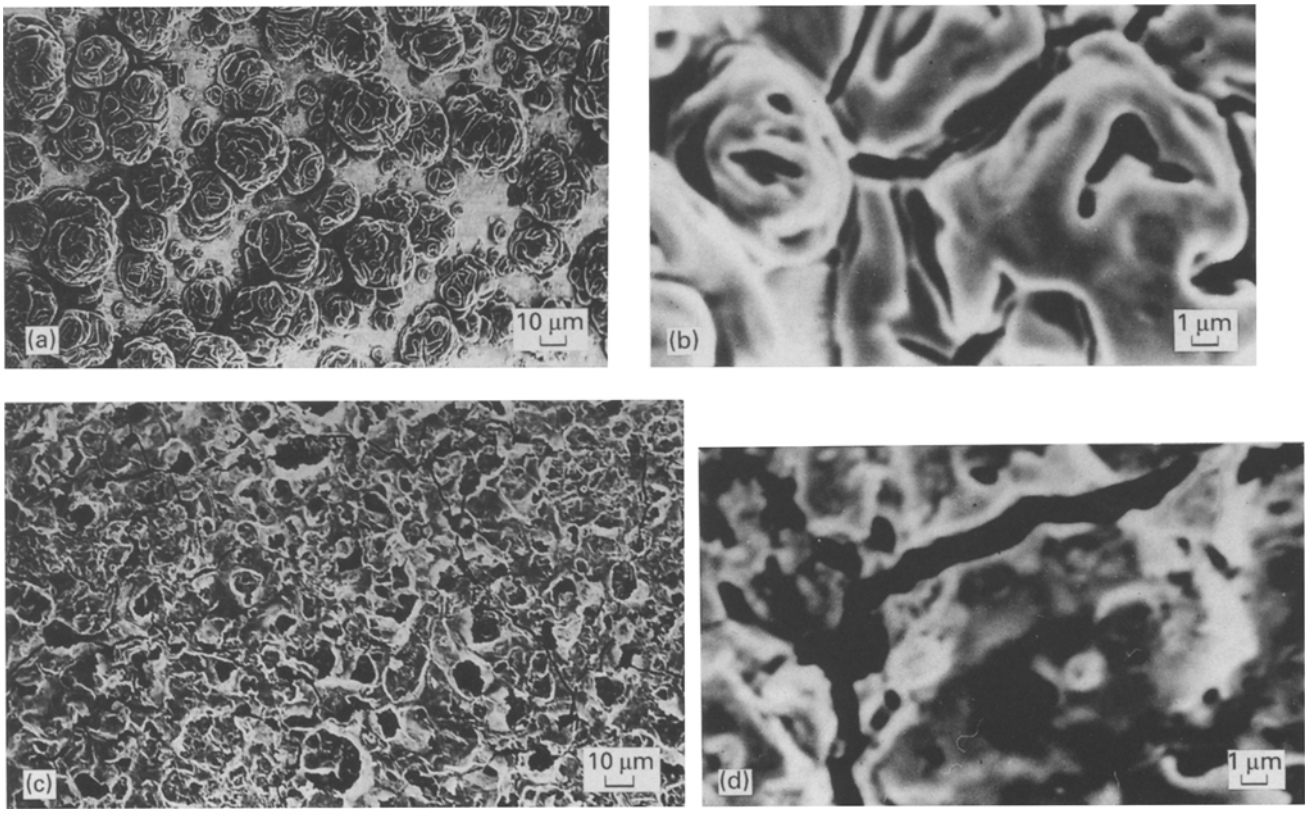

Fig. 1. SEM micrographs for (a) and (b) sprayed, and (c) and (d) layer deposited $LaNiO_3$ films on platinum.

(Merck) solution was used as an electrolyte and double-distilled water was used for its preparation and dilution.

The steady state E–log i relationships were obtained in potentiostatic mode, with a PGS 81 potentio–galvano scan (Wenking model). Freshly prepared oxide electrodes were first anodized at 25 mA cm^{-2} for 25 min in 1 M KOH and then used for the polarization experiments. Prior to each experiment, the preanodized oxide electrode was further anodized at the same current density for 15 min to produce an oxygen environment around the working electrode and then brought back to the open-circuit conditions. After 10 min the electrode potential was increased in steps and the steady value of current corresponding to each applied potential was noted.

Cyclic voltammetry was carried out using a bipotentiostat (model RDE4, Pine Instruments Company, USA) connected to an X–Y recorder (Model 2000, Houston Instruments). Before recording the voltammograms, the electrode was invariably cycled for 2–3 min at a scan rate of 50 mV s^{-1}.

3. Results and discussion

3.1. *Morphology*

The scanning electron micrographs of films of $LaNiO_3$ obtained on the platinum by the layer method and by spray pyrolysis are shown in Fig. 1(a)–(d). This figure shows that both types of films are quite uniform and porous, however, their surface morphologies are different. In the case of the sprayed film (Fig. 1(a) and (b)), approximately circular flat porous masses of approximately 20 μm diameter are formed while such structures are absent in the film prepared by the layer method. Furthermore, the latter film (Fig. 1(c) and (d)) exhibits some cracks and appears to be more compact and homogeneous but less porous.

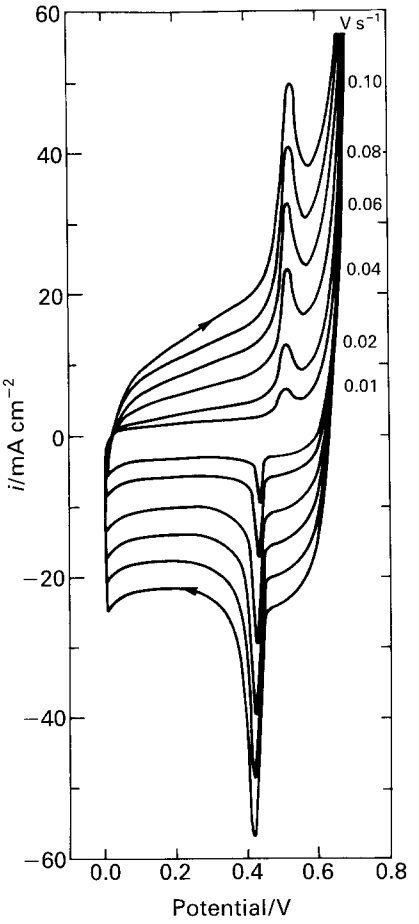

Fig. 2. Cyclic voltammograms for layer deposited $LaNiO_3$ film on platinum in 1 M KOH at various potential scan rates (25° C).

3.2. *Cyclic voltammetry*

The cyclic voltammetric behaviour of a $LaNiO_3$ film on platinum prepared by the layer method was studied in 1 M KOH at varying potential scan rates (Fig. 2). The cyclic voltammograms show the characteristic anodic and cathodic peaks located at 520 ± 15 and 425 ± 5 mV, respectively, corresponding to the redox couple Ni(III)–Ni(II): these were found to be

Table 1. Results of cyclic voltammograms obtained at $LaNiO_3$ films on platinum prepared by layer and spray pyrolysis techniques (25° C)

Scan rate /V s^{-1}	E_{pa} /V	E_{pc} /V	ΔE_p /V	$E^0 = (E_{pa} + E_{pc})/2$ /V	i_{pa} /mA cm^{-2}	i_{pc} /mA cm^{-2}
0.01	0.505	0.410	0.095	0.457	0.425	0.25
	(0.510)	(0.445)	(0.075)	(0.472)	(0.70)	(1.20)
0.02	0.515	0.410	0.105	0.462	0.80	0.425
	(0.515)	(0.435)	(0.080)	(0.475)	(1.50)	(2.15)
0.04	0.520	0.410	0.110	0.465	1.35	0.70
	(0.520)	(0.430)	(0.090)	(0.475)	(2.70)	(3.50)
0.06	0.525	0.405	0.120	0.465	1.875	0.90
	(0.525)	(0.425)	(0.100)	(0.475)	(3.60)	(4.60)
0.08	0.530	0.400	0.130	0.465	2.35	1.025
	(0.530)	(0.420)	(0.110)	(0.475)	(4.50)	(5.50)
0.10	(0.535)	(0.420)	(0.115)	(0.477)	(6.10)	(0.852)

Data shown in parentheses corresponds to the $LaNiO_3$ film electrode (layer).

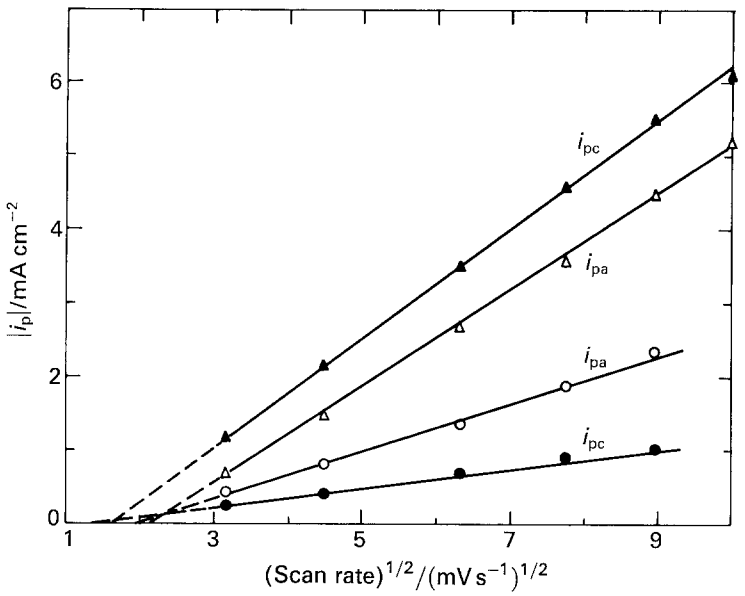

Fig. 3. Variation of anodic and cathodic peak currents as a function of the square root of the scan rate. (△) and (▲) $LaNiO_3$ (layer); (○) and (●) $LaNiO_3$ (spray).

unaffected by repetitive potential steps. Experiments were carried out between 0 and 0.6 V in 1 M KOH. Similar cyclic voltammograms showing two current peaks ($E_{pa} = 535 \pm 10$ mV, $E_{pc} = 425 \pm 5$ mV) were also found on sprayed $LaNiO_3$ film. It is noteworthy that such sharply defined peaks have, to our knowledge, never been reported with massive pellets of $LaNiO_3$.

The effect of scan rate on the peak position and its height was also examined (Fig. 2) and the results are given in Table 1. This table shows that the anodic peak potential shifts slightly in the positive direction with increasing potential scan rate, the shift in potential being ~ 20 mV with a ten fold increase in scan rate, while the cathodic peak potentials remain practically constant. The anodic (i_{pa}) and cathodic (i_{pc}) peak currents were found to vary linearly with the square root of scan rate (Fig. 3), showing that the redox processes are diffusion controlled.

It has been noted that the height and the position of the redox peaks were not affected as the anodic potential limit of 0.6 V was extended to 0.7 V into the oxygen evolution region. This indicates that oxygen evolution occurs on an oxide surface fully oxidized to Ni(III).

3.3. *Roughness factors*

Potential ranges of 0.335–0.375, 0.350–0.400 and 0.400–0.450 V were used in the determination of the double layer capacitance. The latter is 50 mV

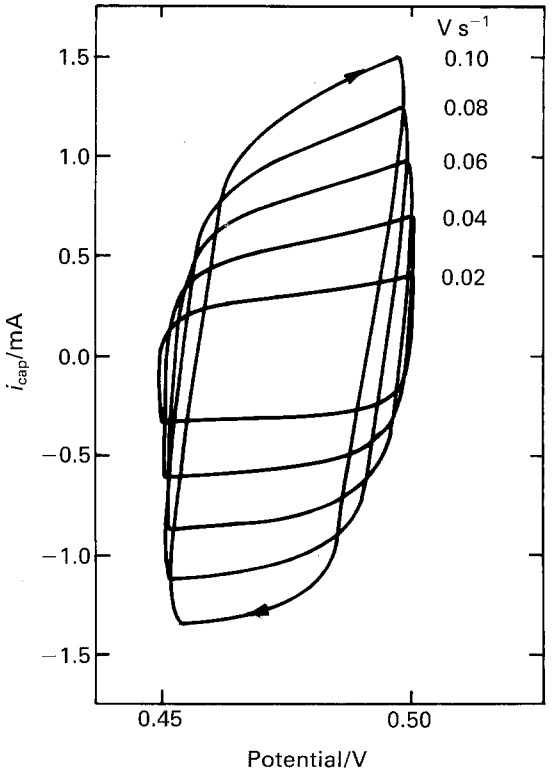

Fig. 4. Cyclic voltammograms for layer deposited $LaNiO_3$ film ($S = 0.5$ cm^2), limited to the potential range of 0.40–0.45 V, in 1 M KOH (25° C).

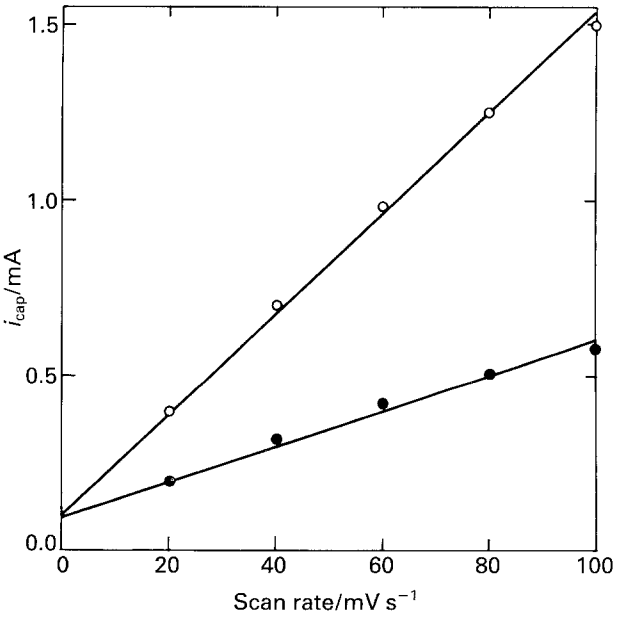

Fig. 5. Capacity current against scan rate plots for sprayed and layer deposited $LaNiO_3$ films ($S = 0.5$ cm^{-2}) in 1 M KOH (25° C). (○) $LaNiO_3$ (layer); (●) $LaNiO_3$ (spray).

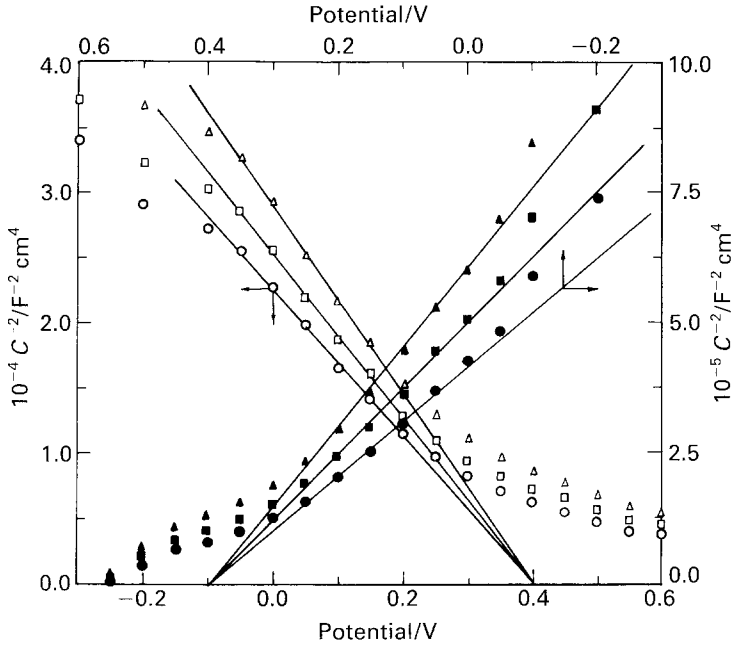

Fig. 6. Mott–Schottky plots for sprayed and layer deposited $LaNiO_3$ film in 1 M KOH at various frequencies (25° C); (○) and (●) 7.9 Hz; (△) and (▲) 12.6 Hz; (□) and (■) 19.9 Hz. (○, □, △) layer; (●, ■, ▲) spray.

more positive than the flat-band potential (see below). In these small potential regions, cyclic voltammograms of film electrodes in 1 M KOH were recorded at various potential scan rates, as shown in Fig. 4 in the case of a $LaNiO_3$ film obtained by the layer method. Values of the double layer capacitance (C_{dl}) were obtained from the slope of the linear plot, i_{cap} against scan rate (Fig. 5), where i_{cap} is the charging current. C_{dl} was found to be about the same, i.e. $\sim 10^4\,\mu F\,cm^{-2}$, whatever the potential range used. These were found to be 1.0×10^4 and $2.8 \times 10^4\,\mu F\,cm^{-2}$ for the sprayed and layered $LaNiO_3$ films, respectively. The corresponding values of the roughness factor were 170 and 470, respectively. The roughness factor was calculated by assuming a double layer capacitance of $60\,\mu F\,cm^{-2}$ for a smooth oxide surface [18, 25, 26]. A similar order of the roughness factor was also reported for several perovskites prepared by high temperature solid-state reactions [24–26]. Further, an intercept on the i_{cap} axis at ~ 0.1 mA in Fig. 5 indicates the occurrence of faradaic processes such as electrochemical adsorption of OH^- ions during the cyclic runs.

3.4. *Mott–Schottky plot*

The Mott–Schottky plots determined on the oxide films at frequencies 7.9, 17.6 and 19.9 Hz are shown in Fig. 6. Frequencies up to 500 Hz were used. The negative slope of the plot between −0.05 and 0.25 V (Hg/HgO) indicates a p-type surface. The value of the flat-band potential was close to 0.40 V in each case, which was higher than the value (0.15–0.2 V) obtained by other methods [24–26]. The observed deviation at higher anodic potentials (> 0.3 V) may be ascribed to the increasing specific adsorption of OH^- ions on the electrode surface [24].

3.5. *Tafel plots*

The *iR*-corrected *E* against log *i* plots for the oxygen evolution reaction were determined on oxide film electrodes at varying concentrations of KOH as shown in Figs 7 and 8. The geometrical surface area of the electrode was used to express the current density. The resistance of the electrolyte plus the oxide film was determined in each experiment by

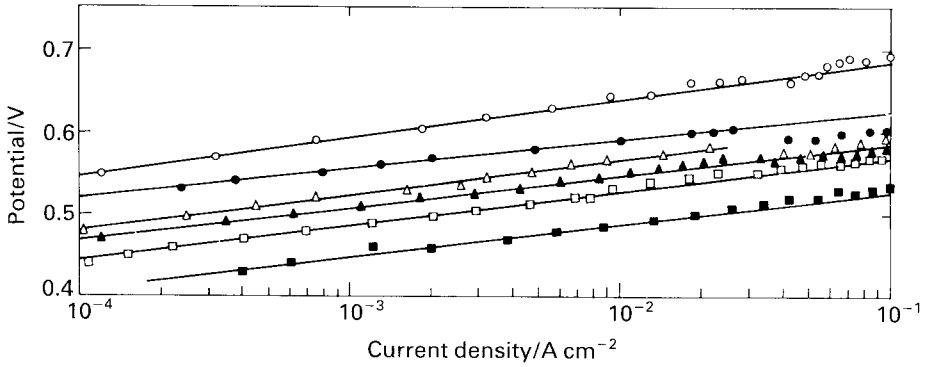

Fig. 7. Tafel plots for oxygen evolution on sprayed $LaNiO_3$ film in different concentrations of KOH (25° C); (○) 1 M; (●) 2 M; (△) 3 M; (▲) 4 M; (□) 5 M; (■) 30 w/o.

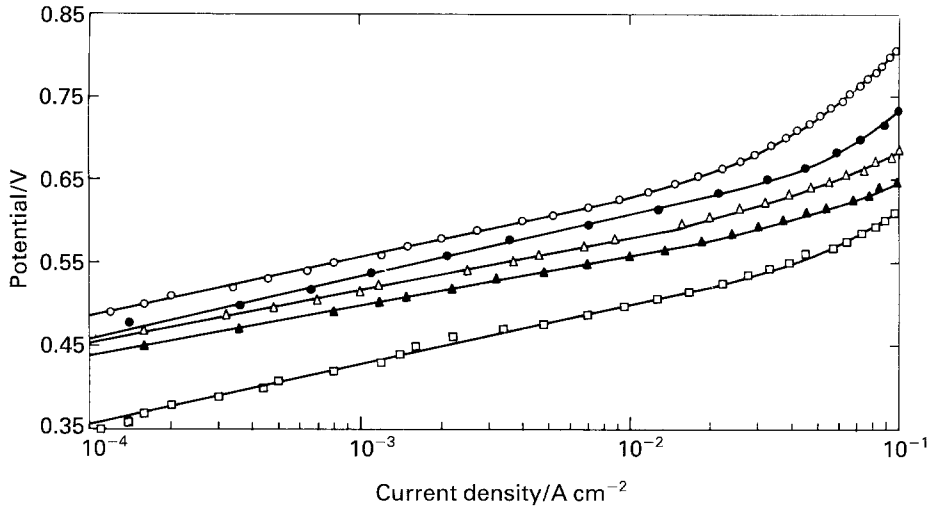

Fig. 8. Tafel plots for oxygen evolution on layer deposited $LaNiO_3$ film in different concentrations of KOH (25° C); (○) 1 M; (●) 2 M; (△) 3 M; (▲) 4 M; (□) 30 w/o.

impedance measurements, and values ranged between 2.5 Ω and 0.5 Ω.

Curves for sprayed $LaNiO_3$ shown in Fig. 7 exhibit a single Tafel slope of about 40 mV decade^{-1} regardless of OH^- concentration. Thus, the results demonstrate a single mechanism for oxygen evolution in the whole range of applied anodic potentials. On the other hand, under the given experimental conditions, the $LaNiO_3$ electrode prepared by the layer method showed a higher Tafel slope (65–70 mV decade^{-1}). The reaction order with respect to OH^- on the sprayed film electrode was found to be twice the reaction order on the layered film (respectively about 2.2 and 1.2).

The $LaNiO_3$ electrode for oxygen evolution was also studied by Bockris *et al.*, where the oxide catalyst was synthesized by a high temperature solid state reaction [24–26] of appropriate mixtures of binary oxides and also by a coprecipitation technique [23]. The latter technique resulted in a low Tafel slope of 43 mV decade^{-1}, while the former resulted in 65–130 mV decade^{-1}. The reaction order with respect to OH^- was observed to be unity, regardless of the preparation method. On the other hand, the same catalyst prepared by us using spray pyrolysis in thin film form showed second order kinetics in OH^- and a single Tafel region of ~ 40 mV decade^{-1} in the whole current density region. First order kinetics in OH^- and a Tafel slope of ~ 65 mV decade^{-1} were obtained on films prepared by the layer method. Second order kinetics were also observed on $La_{1-x}Sr_xCoO_3$ ($x = 0.2, 0.4$) by Matsumoto *et al.* [27] while Kobussen and Mesters [28] and Brockris and Otagawa [24] found first order kinetics in the case of a number of cobaltates. On oxides with the general formula $NiLn_2O_4$ (Ln : La, Pr, Nd) Fiori *et al.* [35], have found a Tafel slope of 40 mV decade^{-1} and a reaction order against OH^- of ~ 1.9, below 100 mA cm^{-2}, but a higher Tafel slope (120 mV dec^{-1}) and a lower reaction order (~ 1) above 100 mA cm^{-2} to 1 A cm^{-2}. This region of higher current densities was not explored in this preliminary work.

Values of the kinetic parameters determined on the $LaNiO_3$ electrode prepared by different methods are shown in Table 2. This Table shows that the values of the exchange current density is minimum for the sprayed $LaNiO_3$ film and maximum for the layer electrode. Based on values of the overpotential at 10 mA cm^{-2} and 100 mA cm^{-2} shown in Table 2 at 25° C, $LaNiO_3$ electrodes in the form of thin films are more active than electrodes obtained by high temperature solid state reactions [24–26]. Further, the sprayed $LaNiO_3$ film electrode is more active than the layer electrode but is less active than the $LaNiO_3$

Table 2. Electrode kinetic parameters for oxygen evolution on $LaNiO_3$ in 1 M KOH at 25° C

Electrode	*Roughness factor*	*Tafel slope* /mV decade^{-1}	*p(OH)*	$i_0 \times 10^9$ *A cm*$^{-2}$ (*Based on geometrical surface area*)	*η/V*	
					10^{-2} A cm^{-2}	10^{-1} A cm^{-2}
$LaNiO_3$ (spray)	170	45	2.2	0.07	~ 0.337	~ 0.387
$LaNiO_3$ (layer)	470	65	1.2	340	~ 0.330	~ 0.410
$LaNiO_3$ (high temp. reaction)	750	65	1.1	59	~ 0.380	~ 0.510
$LaNiO_3$ (coprecipitation)	5600	43	0.95	6.3	~ 0.265	~ 0.315

electrode obtained by a co-precipitation technique [23]. However, due to the second order kinetics in OH^- a better performance of the sprayed $LaNiO_3$ film anode is expected in highly concentrated alkaline solutions. Thus tests were also made in 30 w/o KOH (Figs 7 and 8) which gave current density of 100 mA cm^{-2} at overpotentials of 280 and 360 mV on sprayed and layer deposited $LaNiO_3$, respectively.

Cyclic voltammograms demonstrate that the oxygen evolution reaction occurs at the oxidized Ni(III) surface [36], as the anodic peak corresponding to this active species is followed by oxygen evolution. In view of this, and to account for the observed kinetic parameters, we suggest the mechanism for oxygen evolution on $LaNiO_3$ films as shown in steps 1–3 which comprise Scheme 1. Similar mechanisms for oxygen evolution involving a physisorbed hydrogen peroxide intermediate have also been proposed on some oxygen evolving anodes [20, 24, 38–39] in alkaline medium.

Scheme 1:

$$\mathrm{Ni(III) + OH^- \overset{k_1}{\rightleftharpoons} Ni(III)OH + e^-} \quad (1)$$

$$\mathrm{Ni(III)OH + OH^- \xrightarrow[k_2]{\text{rds}} Ni(III).H_2O_2 + e^-} \quad (2)$$

$$\mathrm{2Ni(III).H_2O_2 \xrightarrow[k_3]{\text{fast}} 2Ni(III) + 2H_2O + O_2} \quad (3)$$

Under Langmuir adsorption conditions, the overall current density for oxygen evolution is,

$$i = nF\overleftarrow{i} = nF\overleftarrow{k}_2\theta_1 C_{OH^-} \exp\left[(1-\beta)\frac{F\Delta\phi}{RT}\right] \quad (4)$$

where θ_1 is the fractional surface coverage by the adsorbed intermediate Ni(III)OH. Other symbols have their usual meanings.

Applying quasiequilibrium conditions to step 1 of Scheme 1 and assuming the total surface coverage ($\theta_T = \theta_1 + \theta_2$) by adsorbed intermediates, Ni(III)OH and $Ni(III).H_2O_2$ under Langmuir adsorption conditions, the value of θ_1 is

$$\theta_1 = K_1 C_{OH^-} \exp\left(\frac{F\Delta\phi}{RT}\right) \quad (5)$$

where $K_1 (= \overleftarrow{k}_1/\overrightarrow{k}_1)$ is the equilibrium constant for the adsorption process (step 1). Thus, the overall current density for oxygen evolution becomes

$$i = nF\overleftarrow{k}_2 K_1 C_{OH^-}^2 \exp\left[(2-\beta)\frac{F\Delta\phi}{RT}\right] \quad (6)$$

$$= 2F\overleftarrow{k}_2 K_1 C_{OH^-}^2 \exp\left[(2-\beta)\frac{F\Delta\phi}{RT}\right] \quad (7)$$

Equation 7 demonstrates a Tafel slope of ~ 40 mV $decade^{-1}$ and the reaction order 2 in OH^- ion concentration. These results are in accord with the observed electrode kinetic data for the sprayed $LaNiO_3$ film.

The kinetic parameter for the layer deposited $LaNiO_3$ film can be interpreted by considering the involvement of Temkinian behaviour of the adsorption process. In this, θ_T influences the heats of adsorption and, hence, the free energies of activation. Such an adsorption has already been considered by Thomas [40] and Parsons [41] in the case of hydrogen electrode reactions and by Conway and Gileadi [42], Conway and Salomon [43], and Bockris and Otagawa [24], for the oxygen evolution reaction.

Thus, under Temkin adsorption conditions, an expression for the overall current density for oxygen evolution can be written as

$$i = nF\overleftarrow{k}_2\theta_1 C_{OH^-} \exp[(1-\alpha)r\theta_T/RT] \times \exp\left[(1-\beta)\frac{F\Delta\phi}{RT}\right] \quad (8)$$

where r is a coefficient determining the variation of heat of adsorption with $\theta_T\alpha$ as the symmetry factor.

Assuming a quasiequilibrium state for step 1:

$$\left(\frac{\theta_1}{1-\theta_T}\right) = K_1 C_{OH^-} \exp\left(\frac{-r\theta_T}{RT}\right) \exp\left(\frac{F\Delta\phi}{RT}\right) \quad (9)$$

At intermediate coverage ($0.2 < \theta_T < 0.8$), the major effect of coverage will be shown by the exponential term only. Thus, taking the logarithm of Equation 9 and neglecting the term $\ln(\theta_1/1-\theta_T)$:

$$\theta_T = \frac{RT\ln(K_1 C_{OH^-}) + F\Delta\phi}{r} \quad (10)$$

Now, putting the value of θ_T in Equation 8, the expression for overall current density becomes

$$i = 2F\overleftarrow{k}_2\theta_1 C_{OH^-} \exp\left[-(RT\ln K_1 + RT\ln C_{OH^-} + F\Delta\phi)\left(\frac{1-\alpha}{RT}\right)\right] \exp\left[(1-\beta)\left(\frac{F\Delta\phi}{RT}\right)\right] \quad (11)$$

Assuming that θ_1 is relatively invariant under intermediate coverage conditions, Equation 11 gives values of the Tafel slope and reaction order ~ 60 mV $decade^{-1}$ and ~ 1.5, respectively, with α and β each being approximately 0.5. The Tafel slope value and the reaction order, thus calculated, are in close agreement with the experimental values found for oxygen evolution on the $LaNiO_3$ films electrode obtained by the layer method.

4. Conclusions

This preliminary work was mainly directed towards the behaviour of homogeneous thin films of $LaNiO_3$, with a special attention to films prepared by carefully controlled spray pyrolysis. Spray pyrolysis is seen as being able to yield fundamental informations on the properties of materials, compared to the other methods of preparation. The $LaNiO_3$ film electrode obtained by the method of spray pyrolysis has shown very interesting electrode kinetic features. It displays remarkably well defined (CV) surface redox peaks of the Ni(III)/Ni(II) couple in contrast with massive electrodes of this material. The Tafel slope, as well as the nature of the Tafel lines obtained on this film

electrode are found to be very similar to those found on $LaNiO_3$ electrodes synthesized by the hydroxide coprecipitation technique. The latter is presently considered as one of the best electrocatalysts for oxygen evolution. The work needs to be completed in further studies by experiments at higher current densities and by long term stability tests. The current density, being second order in OH^-, the sprayed $LaNiO_3$ electrode may work better than the $LaNiO_3$ anode in commercial electrolysis cell solutions, provided its electrochemically active surface area, which is found to be approximately 33 times smaller than the active surface area of the latter electrode, is improved. Attempts are continuing to increase the active surface area of the catalyst in thin film form.

Acknowledgements

The support of this work (Project 408-3) by the Indo-French Centre for the Promotion of Advanced Research (Centre Franco-Indien pour la Promotion de la Recherche Avancée) New Delhi, India, is gratefully acknowledged.

References

[1] H. Wendt and G. Imarisio, *J. Appl. Electrochem.* **18** (1988) 1.
[2] L. Brossard and J.-Y. Huot, *ibid.* **19** (1989) 882.
[3] H. Wendt and H. Hofmann, *ibid.* **19** (1989) 605.
[4] L. Chen and A. Lasia, *J. Electrochem. Soc.* **138** (1991) 3321.
[5] D.E. Hall, *ibid.* **128** (1981) 740; *ibid.* **129** (1982) 310.
[6] P. Rasiyah and A.C.C. Tseung, *ibid.* **130** (1983) 2384.
[7] A. M. Couper, D. Pletcher and F.C. Walsh, *Chem. Rev.* **90** (1990) 837.
[8] P. W. T. Lu and S. Srinivasan, *J. Electrochem. Soc.* **125** (1978) 1416.
[9] A. C. C. Tseung and S. Jasem, *Electrochim. Acta* **22** (1977) 31.
[10] L. M. Volchkova and A. I. Krasil'shchikov, *Zh. Fiz. Khim.* **23** (1949) 441.
[11] S. Gottesfeld and S. Srinivasan, *J. Electroanal. Chem.* **86** (1978) 89.
[12] T. A. Liederbach, A. M. Greenberg and V. H. Thomas, *in* 'Modern Chlor–Alkali Technology', Vol. 1, (edited by M. Coulter), Ellis Horwood, Chichester (1980) p. 145.
[13] J. De Carvalho, G. Tremilliosi-Filho, L. A. Avaca and E. R. Gonzalez, *Int. J. Hydrogen Energy* **14** (1989) 161.
[14] T. Kenjo, *J. Electrochem. Soc.* **132** (1985) 383; *Electrochim. Acta* **31** (1986) 76.
[15] D. E. Hall, *J. Appl. Electrochem.* **14** (1984) 107.
[16] P. Rasiah and A. C. C. Tseung, *J. Electrochem. Soc.* **130** (1983) 365.
[17] C. Iwakura, A. Honji and H. Tamura, *Electrochim. Acta* **26** (1981) 1319.
[18] R. N. Singh, J. F. Koenig, G. Poillerat and P. Chartier, *J. Electrochem. Soc.* **137** (1990) 1408.
[19] R. Boggio, A. Carugati and S. Trasatti, *J. Appl. Electrochem.* **17** (1987) 828.
[20] R. N. Singh, M. Hamdani, J. F. Koenig, G. Poillerat, J. L. Gautier and P. Chartier, *J. Appl. Electrochem.* **20** (1990) 442.
[21] M. R. Tarasevich and B. N. Efremov, 'Electrodes of Conductive Metallic Oxide', Part A (edited by S. Trasatti), Elsevier, Amsterdam (1981) p. 221.
[22] L. D. Burke and M. M. McCarthy, *J. Electrochem. Soc.* **135** (1988) 1175.
[23] T. Otagawa and J. O'M. Bockris, *J. Electrochem. Soc.* **192** (1982) 2391.
[24] *Idem*, *J. Phys. Chem.* **87** (1983) 2960.
[25] J. O'M. Bockris, T. Otagawa and V. Young, *J. Electroanal. Chem.* **150** (1983) 633.
[26] J. O'M. Bockris and T. Otagawa, *J. Electrochem. Soc.* **131** (1984) 290.
[27] V. Matsumoto, H. Manabe and E. Sato, *J. Electrochem. Soc.* **127** (1980) 811.
[28] A. G. C. Kobussen and C. M. A. M. Mesters, *J. Electroanal. Chem.* **115** (1980) 131.
[29] E. J. M. O'Sullivan and E. T. Calvo, *in* 'Comprehensive Chemical Kinetics', Vol. 27, (Electrode Kinetic Reactions), (edited by R. G. Compton), Elsevier, Amsterdam (1987) p. 294.
[30] A. C. C. Tseung and H. L. Bevan, *J. Mater. Sci.* **5** (1970) 604; J. Kelly, D. B. Hibbert and A. C. C. Tseung, *J. Mater. Sci.* **13** (1978) 1053; D. B. Hibbert and A. C. C. Tseung, *J. Mater. Sci.* **14** (1979) 2665.
[31] G. Karlsson, *J. Power Sources* **10** (1983) 319.
[32] V. Matsumoto and E. Sato, *Denki Kagaku* **51** (1983) 783.
[33] A. Daghetti, G. Lodi and S. Trasatti, *Mater. Chem. Phys.* **8** (1983) 1.
[34] L. Bahadur, M. Hamdani, J. F. Koenig and P. Chartier, *Sol. Energy Mater.* **14** (1986) 107.
[35] G. Fiori, C. M. Mari, B. Perra, L. Vago and P. Vitali, EC Report EUR 6783, Hydrogen Energy Vector (1980), pp. 223–239 and references therein.
[36] S. K. Tiwari, K. L. Anitha and R. N. Singh, *J. Electroanal. Chem.* **319** (1991) 263.
[37] M. Hamdani, J. F. Koenig and P. Chartier, *J. Appl. Electrochem.* **18** (1988) 568.
[38] R. F. Scarr, *J. Electrochem. Soc.* **116** (1969) 1526.
[39] A G. C. Kobussen and G. H. J. Broers, *J. Electroanal. Chem.* **126** (1981) 221.
[40] J. G. N. Thomas, *Trans. Faraday Soc.* **57** (1961) 1603.
[41] R. Parsons, *ibid.* **54** (1958) 1053.
[42] B. E. Conway and E. Gileadi, *ibid.* **58** (1962) 2493.
[43] B. E. Conway and M. Salomon, *Electrochim. Acta* **9** (1964) 1599.